Junction barrier Schottky rectifier with an improved P-well region*

Wang Ying(王 颖)†, Li Ting(李 婷), Cao Fei(曹 菲), Shao Lei(邵 雷), and Chen Yu-Xian(陈宇贤)

College of Information and Communication Engineering, Harbin Engineering University, Harbin 150001, *China*

(Received 16 March 2012; revised manuscript received 16 May 2012)

A junction barrier Schottky (JBS) rectifier with an improved P-well on 4H–SiC is proposed to improve the V_F–I_R trade-off and the breakdown voltage. The reverse current density of the proposed JBS rectifier at 300 K and 800 V is about 3.3×10^{-8} times that of the common JBS rectifier at no expense of the forward voltage drop. This is because the depletion layer thickness in the P-well region at the same reverse voltage is larger than in the P^+ grid, resulting in a lower spreading current and tunneling current. As a result, the breakdown voltage of the proposed JBS rectifier is over 1.6 kV, that is about 0.8 times more than that of the common JBS rectifier due to the uniform electric field. Although the series resistance of the proposed JBS rectifier is a little larger than that of the common JBS rectifier, the figure of merit (FOM) of the proposed JBS rectifier is about 2.9 times that of the common JBS rectifier. Based on simulating the values of susceptibility of the two JBS rectifiers to electrostatic discharge (ESD) in the human body model (HBM) circuits, the failure energy of the proposed JBS rectifier increases 17% compared with that of the common JBS rectifier.

Keywords: Schottky rectifier, breakdown voltage, forward voltage drop, reverse current density

PACS: 85.30.Tv, 85.30.De, 85.30 **DOI:** 10.1088/1674-1056/21/12/128503

1. Introduction

The commercially available power rectifiers are either Schottky diodes or P–I–N diodes.[1,2] The optimum design of the Schottky diode requires both a low forward voltage drop (V_F) and a low reverse leakage current (I_F) simultaneously. However, a low barrier height can induce low V_F, while I_R increases for both a lower barrier height and a barrier height lowering effect with the increase of reverse voltage.[3] In recent years, some Schottky diodes have been investigated to optimize the V_F–I_R trade-off such as junction barrier Schottky (JBS) rectifiers, merged P–i–N Schottky (MPS) rectifiers, and trench MOS-barrier Schottky (TMBS) rectifiers.[4] Several 4H–SiC JBS rectifiers have been treated, such as by reducing the forward voltage drop through reducing the surface damage during high temperature annealing with an AlN cap,[5] by increasing the breakdown voltage through improving the passivation layer,[6] and by reducing the reverse leakage current through using linear and honeycombed P^+ grids of the JBS rectifier.[7] However, the V_F–I_R trade-off in a JBS rectifier is a strong function of P^+ grid size and the grid spacing, because they control the forward conduction area, the pinch-off voltage and the depletion region. In this paper, the V_F–I_R trade-off and the breakdown voltage of a JBS rectifier with the P-well are improved. Furthermore, the susceptibility of the JBS rectifier with the P-well to electrostatic discharge (ESD) in the human body model (HBM) circuits has also been discussed.

2. Device structure and operation concept

The schematic diagrams of the two JBS rectifiers are shown in Fig. 1. The proposed JBS rectifier consists of Schottky contacts and P^+ girds, which is the same as the common JBS rectifier in the sense of structure. While the P^+ girds in the proposed structure are surrounded by P-wells. The forward voltage drop of the proposed JBS rectifier is determined by the resistance of the drift region, the Schottky barrier height, and the relative area of Schottky contacts to the p-type regions, which is similar to the forward voltage

*Project supported by the Program for New Century Excellent Talents in University, China (Grant No. NCET-10-0052) and the Fundamental Research Funds for the Central Universities of China (Grant No. HEUCFT1008).

†Corresponding author. E-mail: wangying7711@yahoo.com

© 2012 Chinese Physical Society and IOP Publishing Ltd

drop of the common JBS rectifier.[8]

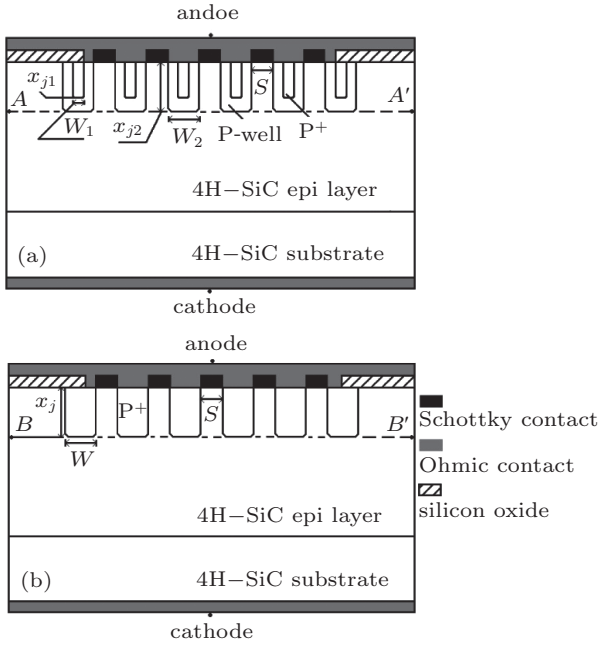


Fig. 1. Cross sections of the (a) proposed and (b) common JBS rectifier.

In the off state of the proposed JBS rectifier, the N-epi layer is depleted by the neighbouring P-well as well as by the P^+ grids. The depletion between the N-epi layer and P-well causes an increase in space charge in the P-well, resulting in uniform electric field distribution and the increase of breakdown voltage. It should be noted that the edge terminations of the two JBS rectifiers are the same as the respective P type region which can be formed without additional process cost.

The proposed process flow of major steps for fabricating the proposed JBS rectifier is shown in Fig. 2. The starting material is an N^+-type 4H–SiC substrate with a 10-μm N-epi layer doped to 1×10^{16} cm^{-3}. After cleaning the wafer (Fig. 2(a)), N-type 4H–SiC (Fig. 2(b)) is etched, a p-type epilayer with a doping concentration of 1×10^{17} cm^{-3} is grown, and a P^+-type epi layer with a doping concentration of 1×10^{19} cm^{-3} obtained by chemical vapor deposition (CVD) (Figs. 2(c) and 2(d)) and ion implantation for Ohmic contact (Fig. 2(e)) are used. Removing the implantation mask material, the sample is annealed in argon ambient in a high-temperature furnace and then a high-quality thermal oxide is used for passivation. Subsequently, Schottky contact openings are formed by selective reactive ion etching and then immediately loaded into metallization (Fig. 2(f)).

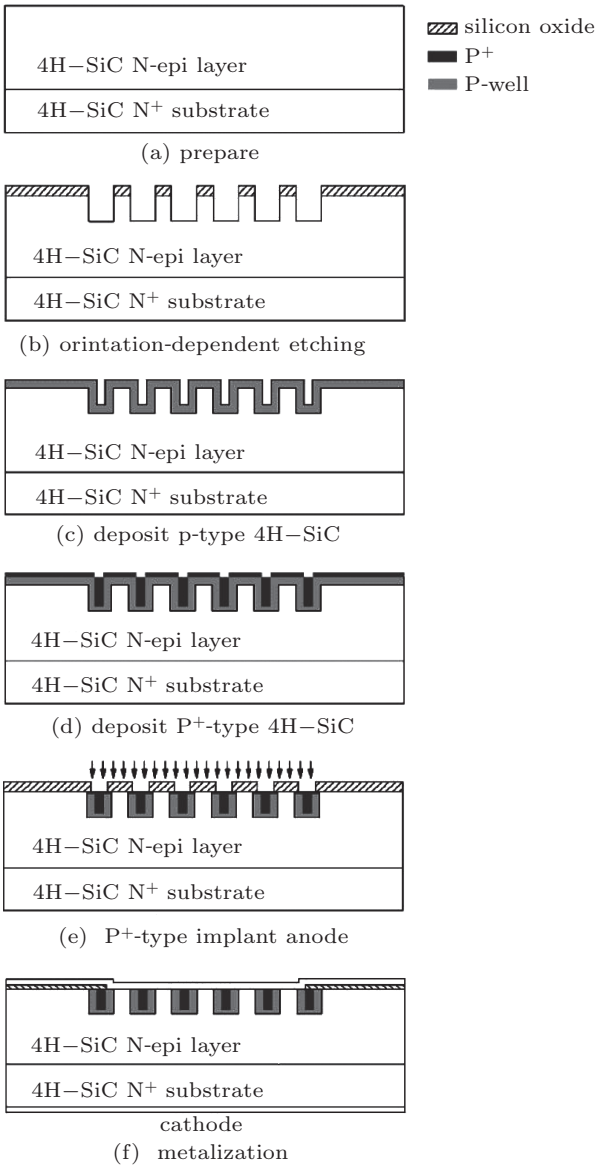


Fig. 2. Proposed fabrication procedure of the proposed JBS rectifier.

The performances of the two JBS rectifiers in this work are investigated with Silvaco TCAD. The 4H–SiC parameters used in the calculation are listed in Table 1.[9–11] The mobility is calculated using the Caughey–Thomas model. In the breakdown model, electron and hole impact ionization coefficients are related by

$$\alpha_{n(p)} = a_{n(p)} \exp(-b_{n(p)}/E), \tag{1}$$

where E is the electric field; $a_{n(p)}$ and $b_{n(p)}$ are constants, i.e., $a_p = 3.25 \times 10^6$ cm^{-1}, $a_n = a_p/40$, $b_n = b_p = 1.79 \times 10^7$ V/cm.[12] Finally, the optimum device parameters used in the simulation for the two JBS rectifiers are given in Table 2.

Table 1. 4H–SiC parameters used in the two JBS rectifiers.

Property	4H–SiC
Breakdown electric field, $E_{\rm V}$/(kV/cm)	2200
Band gap at 300 K, $E_{\rm g300}$/eV	3.26
Relative dielectric constant, ε	9.7
Doping coefficient of mobility, α	0.76
Maximum mobility, $\mu_{\rm max}$/(cm^2/V·s)	950
Coefficient of $\mu_{\rm max}$, $\gamma_{\mu\,\rm max}$	−2.4
Minimum mobility, $\mu_{\rm min}$/(cm^2/V·s)	40
Coefficient of $\mu_{\rm min}$, $\gamma_{\mu\,\rm min}$	−0.5
Maximum saturated velocity, $v_{s\rm max}$(cm/s)	4.77×10^7

Table 2. Structural parameters of the two JBS rectifiers.

Parameters	Proposed JBS	Common JBS
P$^+$ grids width, W_1	1 μm	3 μm
P-well width, W_2	3 μm	–
P$^+$ grids depth, X_{j1}	2.5 μm	3 μm
P-well depth, X_{j2}	3 μm	–
P$^+$ grids doping, $N_{\rm d1}$	10^{19} cm^{-3}	10^{19} cm^{-3}
P-well doping, $N_{\rm d2}$	10^{17} cm^{-3}	–
Silicon oxide thickness	0.1 μm	0.1 μm
4H–SiC epi layer thickness	10 μm	10 μm
4H–SiC epi layer doping	10^{16} cm^{-3}	10^{16} cm^{-3}
P-well spacing, S	2 μm	2 μm
Schottky barrier height	1 eV	1 eV

3. Simulation results and discussion

Figure 3 shows the dependencies of breakdown voltage (at 1 A/cm^2) of proposed JBS rectifier on the depth of the P$^+$ grid at different values of X_{j1} and X_{j2}. It is known that the proposed JBS rectifier with a 3-μm P-well depth and 2.5-μm P$^+$-grid depth can withstand 1.6 kV. While the breakdown voltage (at 1 A/cm^2) of the common JBS rectifier with 3-μm P$^+$-grid depth is only 885 V. As a result, the breakdown voltage of the proposed JBS rectifier is 0.8 times more than that of the common JBS rectifier. It is attributed to the P-well which makes the bulk electric field distribution uniform as shown below. Figure 4 shows the comparison between the electric field distribution of the proposed JBS rectifier in the range from point A to point A' under breakdown voltage and that of the common JBS rectifier in the range from point B to point B'. It reveals that the electric field at the bottom of p-type region of the proposed JBS rectifier is reduced and the one in the middle of P-well is lifted up, while the electric field distribution at the P-well edge becomes uniform. Thus, the electric field concentration at the guard ring edge is relaxed, and the breakdown voltage of the proposed JBS rectifier is increased.

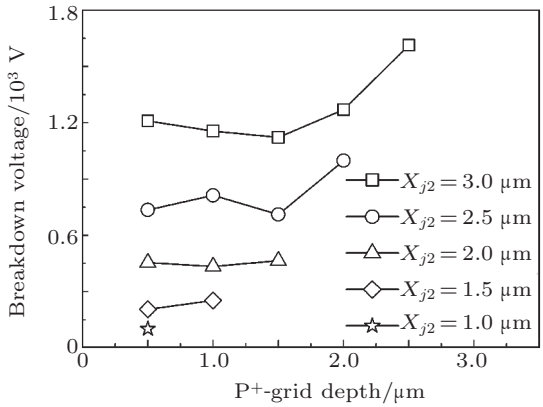


Fig. 3. Breakdown voltages of the proposed JBS rectifier with different values of X_{j1} and X_{j2}.

The variations of breakdown voltage at 1 A/cm^2 about the two JBS rectifiers with $N_{\rm d2}$ and α are simulated and plotted in Fig. 5. As can be seen from this figure, it is clear that the breakdown voltage of the proposed JBS rectifier increases with the value of $N_{\rm d2}$ increasing due to the additional charge suppressing the field effect action. However, a too heavy doping concentration of the P-well (e.g. $N_{\rm d2}=N_{\rm d1}$) will reduce the breakdown voltage because too many p-type dopants at the surface of the P-well are depleted. The ratio W_1/W_2 in Fig. 4 is denoted as α. In particular, when α turns close to 0.5, the breakdown voltage of the proposed JBS rectifier approaches that of the common JBS rectifier with a P$^+$-grid depth of 2.5 μm. It is important to note that the breakdown voltage of the proposed JBS rectifier is maximized when the ratio α equals 0.4. This is due to the fact that the charge compensation between the P-well and the N-epi layers results in the reduction of the electric field at the bottom of the P-well.

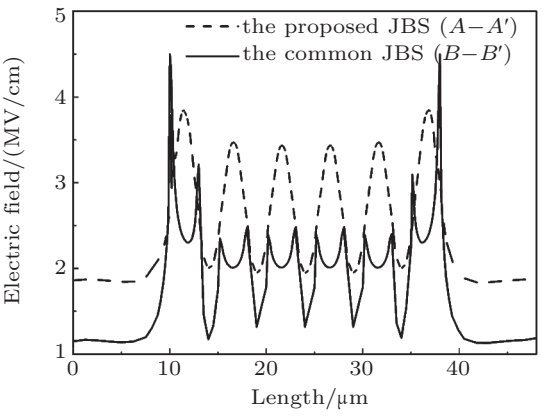


Fig. 4. Electric field distributions of the two JBS rectifiers from point $A(B)$ to point $A'(B')$ under breakdown voltage.

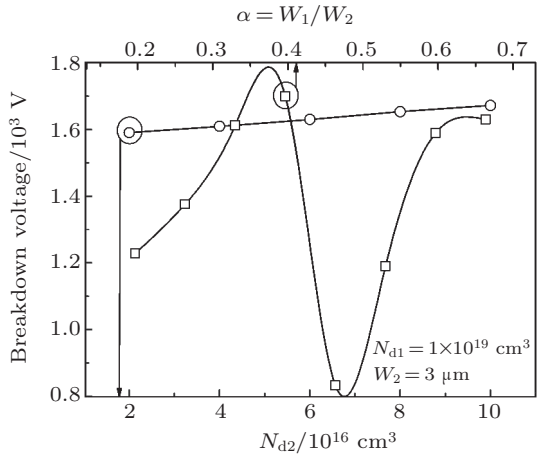


Fig. 5. Breakdown voltages of the proposed JBS rectifier versus N_{d2} and W_1.

Figure 6 displays the reverse current–voltage (I–V) characteristics of the two JBS rectifiers at different temperatures. At 300 K, the breakdown voltage of the proposed JBS rectifier is 1613 V, 1.9 times that of the common JBS rectifier, owing to the uniform electric field distribution as shown in Fig. 3. Besides, the reverse leakage current of JBS is the sum of the spreading current in the depletion due to the diffusion and drift, the tunneling current due to the tunnel effect, and the injection current due to thermionic emission and thermionic field emission. While the depletion layer thickness in the P-well region at the same reverse voltage is larger than that in the P^+ grid, resulting in the lower spreading current and tunneling current. As a result, it is observed that the reverse leakage current densities (at 800 V) of the proposed and common JBS rectifiers at 300 K are 1.22×10^{-9} A/cm^2 and 0.41 A/cm^2, respectively.

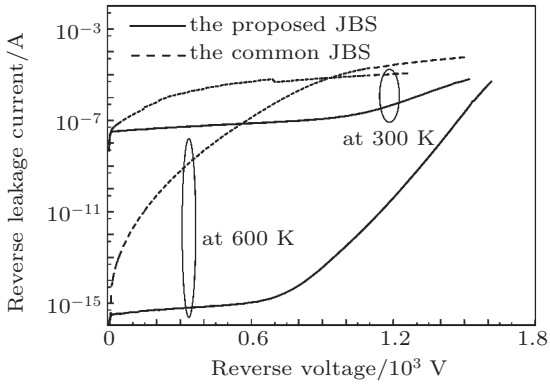


Fig. 6. Reverse I–V characteristics of the two JBS rectifiers at different temperatures.

The reverse leakage current densities (at 800 V) of the proposed and common JBS rectifiers at 600 K are 0.02 A/cm^2 and 1.19 A/cm^2, respectively. As is well known, the reverse leakage current increases significantly with temperature increasing, which accounts for thermionic emission. The impact ionization coefficient with a temperature increase is expressed by Chynoweth's law as

$$\alpha_{n(p)} = a_{n(p)} c(T) \exp(-b_{n(p)} c(T)/E), \qquad (2)$$

with

$$c(T) = \frac{\tanh(h\omega_{op}/2k_B \cdot 300)}{\tanh(h\omega_{op}/2k_B \cdot T)}. \qquad (3)$$

The factor $c(T)$ with the optical phonon energy ($h\omega_{op}$) expresses the temperature dependence of the phonon gas, and the carriers are accelerated with increasing temperature. Here, $h\omega_{op} = 106$ meV, $k_B = 1.38\times10^{-23}$ J·K^{-1}.

As a result, the reverse current density of the proposed JBS rectifier at 300 K and 800 V is about 3.3×10^{-8} times that of the common JBS rectifier. The results obtained show that the depletion region in the P-well for the proposed JBS rectifier widens with the reverse bias voltage increasing. However, the depletion region in the P-well is wider than that in P^+ grid at the same reverse bias voltage due to the lower doping of the P-well. So the reverse leakage current can be reduced by screening the Schottky surface from the high electric field and avoiding the undesired reduction of the Schottky barrier. It is important that PIN-like reverse leakage characteristics are achieved for the proposed JBS rectifier at below 800 V, reaching more than 5.4×10^{10} of the on/off (1 V/–500 V) current ratio, while the common JBS rectifier exhibits a 1.8×10^3 on/off (1 V/–500 V) current ratio.

Figure 7 shows the forward I–V characteristics of the two JBS rectifiers at different temperatures. It is known that the forward voltages of the proposed and common JBS diode at 100 A/cm^2 with a Schottky area of 1×10^{-7} cm^{-2} are about 1.5 V and 1.4 V, respectively. Figure 8 then shows the forward voltage drops of the two JBS rectifiers at different temperatures and different values of forward current density (J_F) with a total area of 4.8×10^{-7} cm^{-2}. At 300 K, the forward voltage drops (at 100 A/cm^2) of the two JBS rectifiers both are about 3.2 V. And at 600 K, the forward voltage drops (at 100 A/cm^2) of the proposed and common JBS rectifiers are 8.4 V and 7.7 V respectively. This is because the active area of the Schottky region is shrunk to a value similar to the active area of the common JBS rectifier. In addition the specific on-resistance increases with increasing temperature, and the specific on-state resistances (at 100 A/cm^2)

of the proposed and common JBS rectifiers at 300 K are 6.9 mΩ·cm^2 and 7.8 mΩ·cm^2, respectively.

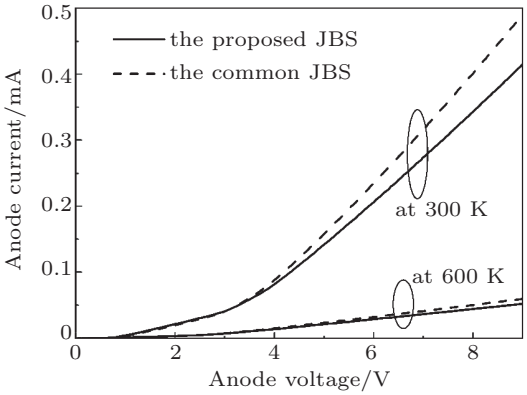


Fig. 7. Forward I–V characteristics of the two JBS rectifiers at different temperatures.

The specific on-resistance (at 100 A/cm^2) of the proposed JBS rectifier increases by about 13% compared with that of the common JBS rectifier at 300 K. This is due to the fact that the resistance in the P-well of the proposed JBS rectifier increases with the increase of contact resistance because of the light doping of the P-well. In addition, the specific on-state resistances (at 100 A/cm^2) of the proposed and common JBS rectifiers at 600 K are 59.1 mΩ·cm^2 and 52.2 mΩ·cm^2, respectively. The reason for this is that the N-epi layer resistance increases with increasing temperature, owing to a decrease in mobility, which can be seen from the following formula:

$$\mu_{\rm n} = \frac{947}{1+\left(\dfrac{N_{\rm D}}{1.94\times10^{17}}\right)^{0.61}}\left(\frac{T}{300}\right)^{-2.15}. \quad (4)$$

Above all, the difference in forward voltage drop between the two JBS rectifiers is lower than 8%. As is well known, the proposed JBS rectifier has a better block capacity and higher figure of merit (FOM) ($BV^2/R_{\rm on,sp}$) which is a quantity used to characterize the performance of a device. The FOMs of the proposed and common JBS rectifiers are 113.5 MW·cm^{-2} and 333.6 MW·cm^{-2}, respectively. Although the series resistance of the proposed JBS rectifier is a little larger than that of the common JBS rectifier, the FOM of the proposed JBS rectifier is about 2.9 times that of the common JBS rectifier.

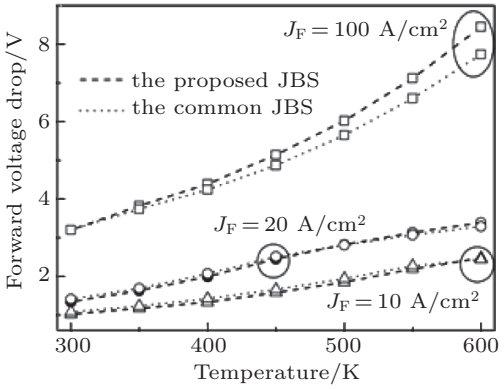


Fig. 8. Forward voltage drops of the two JBS rectifiers at different temperatures and different forward current densities.

In order to test the susceptibility of an electronic device to ESD from human contact, one of the most widely used models is defined in the JEDEC 22-A114-B standard, which specifies the values of 100 pF and 1.5 kΩ, as shown in Fig. 9.[13] The variable resistor in this figure is used as an ideal switching device. Ain addition, the capacitor is charged to a specified high voltage from an external source, and then suddenly discharged through the resistor into an electrical terminal of the device under test. The ESD produces a large current and high electric field in the semiconductor device. Energy released during an ESD event generates "self-heating" in the device and causes a rapid temperature increase. The failure charge and energy can be expressed as follows:[14]

$$Q_{\rm HBM} = C_{\rm S}V_{\rm HBM}, \quad (5)$$

$$E_{\rm HBM} = \int_0^\infty i^2(t)R_{\rm DUT}\,{\rm d}t = 0.5I_{\rm HBM}^2R_{\rm DUT}R_{\rm D}C_{\rm S}. \quad (6)$$

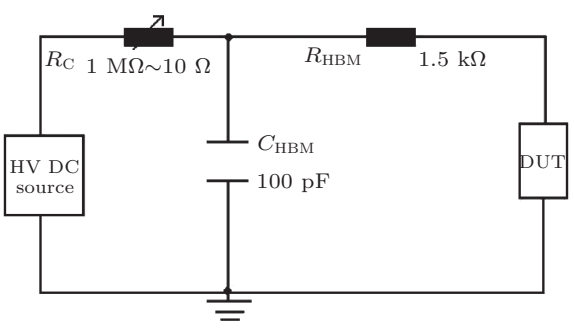


Fig. 9. Equivalent circuit of HBM.

In this work, the temperature of device, which increases with "self-heating", determines whether the failure occurs. In addition, the melting points of aluminum and SiC are about 960 K and 3000 K, respectively. At room temperature of 300 K, the measured

curves of the anode current and global device temperature versus time for the two JBS rectifiers with a total area of 4.8 mm^2 at 300 K are shown in Fig. 10, with the capacitance (C_S) set to be 150 pF in the simulation on transient process.

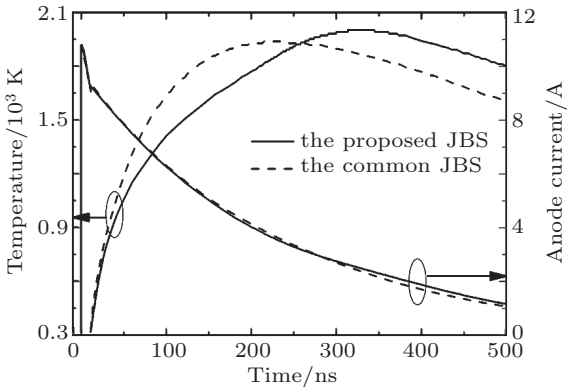


Fig. 10. Curves of anode current and globe device temperature versus time for the two JBS rectifiers.

Table 3. Results of the ESD for the two JBS rectifiers.

Structure	V_{HBM}/kV	I_{HBM}/A	Q_{HBM}/μC	E_{HBM}/μJ
Common JBS	15.98	10.65	2.4	1.83
JBS	16.23	10.82	2.43	2.14

From this figure, the two JBS rectifiers are both discharged because the temperature is higher than 1800 K and the reverse leakage current is close to 1 A due to the thermal breakdown. The values of rise time (90%∼10% I_{HBM}) and the duration time (100%∼37% I_{HBM}) of the two JBS rectifiers are about 5.2 ps and 200 ns, respectively. The values of failure voltage, current, charge, and energy of the two JBS rectifiers are listed in Table 3. The failure energy of the proposed JBS rectifier is 17% more than that of the common JBS rectifier. It is demonstrated through simulations involving parametric variations of the device that the P-well structure has a uniform electric field during the second breakdown.

4. Conclusions

In this paper, an optimized junction barrier Schottky (JBS) rectifier with a P-well on 4H–SiC was proposed and investigated numerically. In the off state of the proposed JBS rectifier, the N-epi layer is depleted by the neighbouring P-well as well as by the P$^+$ grid. The depletion between the N-epi layer and P-well causes an increase in the space charge in the P-well, resulting in uniform electric field distribution, and increasing the breakdown voltage. Although the series resistance of the proposed JBS rectifier is a little larger than that of the common JBS rectifier, the FOM of the proposed JBS rectifier is about 2.9 times that of the common JBS rectifier. In addition, a PIN-like reverse leakage characteristic is obtained for the proposed JBS rectifier, reaching a more than 5.4×10^{10} on/off (1 V/–500 V) current ratio. While the common JBS rectifier exhibits a 1.8×10^3 on/off (1 V/–500 V) current ratio. Based on the simulated values of susceptibility of the two JBS rectifiers to ESD in the HBM circuits, the failure energy of the proposed JBS rectifier is 17% more than that of the common JBS rectifier.

References

[1] Baliga B J 1998 *ISPSD* 5
[2] Funaki T, Kimoto T and Hikihara T 2008 *IEICE Electro. Expr.* **5** 198
[3] Mehrotra M and Baliga B J 1994 *IEEE Trans. Electron. Dev.* **41** 1655
[4] Baliga B J 2001 *Proc. IEEE* **89** 822
[5] Zhu L Chow T P Jones K A and Agarwal A 2006 *IEEE Trans. Electron. Dev.* **53** 363
[6] Brosselard P Banu V Camara N and Pérez-Tomás A 2009 *Mater. Sci. Eng.* B **165** 15
[7] Singh R, Capell D C, Hefner A R, Lai J and Palmour J W 2002 *IEEE Trans. Electron. Dev.* **49** 2054
[8] Hefner A R, Singh R Jr, Lai J S, Berning D W, Bouché S and Chapuy C 2001 *IEEE Trans. Power Elect.* **16** 273
[9] Chang S C, Wang S J, Uang K M and Liou B W 2005 *Solid State Electron.* **49** 437
[10] Roschke M and Schwierz F 2001 *IEEE Trans. Electron. Dev.* **48** 1442
[11] Östling M 2011 *Sci. Chin.: Inf. Sci.* **54** 1087
[12] Raghunathan R and Baliga B J 1999 *Solid State Electron.* **43** 199
[13] Brodbeck T 2000 *Proceedings of the* 22*nd EOS/ESD Symposium*, September 26–28, 2000, Anaheim, CA, America, p. 66
[14] Lee J C, Hoque M A, Croft G D, Liou J J and Bernier J C 2000 *Proceedings of the* 22*nd EOS/ESD Symposium*, September 26–28, 2000, Anaheim, CA, America, p. 97